Journal of Electronic Materials, Vol. 23, No. 8, 1994

Regular Issue Paper

An Accurate and Computationally Efficient Semi-Empirical Model for Arsenic Implants into Single-Crystal (100) Silicon

SHYH-HORNG YANG, STEVEN J. MORRIS, DAVID L. LIM, and AL F. TASCH

Microelectronics Research Center, Department of Electrical and Computer Engineering, The University of Texas at Austin, Austin, TX 78712

ROBERT B. SIMONTON and DENNIS KAMENITSA

Eaton Corporation, Austin, TX 78758

CHARLES MAGEE

Evans East, Plainsboro NJ 08536

GAYLE LUX

Charles Evans and Associates, Redwood City, CA 94063

In this paper is reported an accurate and computationally efficient semi-empirical model based on an extensive set of experimental data for arsenic implants into (100) single-crystal silicon. Experimental and model development details are given, and issues of the measurements are discussed. The newly developed model has explicit dependence on tilt angle, rotation angle, and dose, in addition to energy. Comparisons between the model predictions and experimental data are made in order to demonstrate the accuracy of this model.

Key words: As-implantation, As-profiles in Si, implantation model, Si

INTRODUCTION

Since the mid 1970s, ion implantation has been the major technique for introducing dopant impurity atoms into semiconductor devices in semiconductor manufacturing. Its advantages over other doping methods include accurate dose control, higher purity of the dopant species, reproducibility of the impurity profiles, and its low process temperature. Due to these advantages, it will continue to play an important role in semiconductor device fabrication.

The implanted profile information is necessary as an input for device simulations, for development of models for subsequent thermal processing, and for process optimization and control in fabrication environments. As the physical sizes of devices decrease, very shallow and compact profiles become necessary. Arsenic is widely used in ion implantation to form shallow n-type junctions, because of its heavy mass compared to phosphorus. In order to achieve the best results, the arsenic ions must be implanted at low energies, and care must be taken to select appropriate implant angles to minimize channeling effects. Also, the amount of subsequent thermal processing must be reduced in order to avoid excessive diffusion of the implanted arsenic atoms. This need leads to an increase in the use of rapid thermal annealing, where the final profile will be a strong function of the as-implanted profile. For these reasons, an accurate model for arsenic implants is needed. Also, as the device sizes decrease, the number of process steps continues to increase. This leads to a greater need for a highly accurate model for arsenic implants which is efficient as well.

In this paper are reported the development and results of a highly accurate and computationally efficient model for arsenic implants. The experimental details will be described first, and the selection and evaluation of an appropriate model will be given. The method for extracting parameters will then be explained and finally, the implementation of this model in a process simulator will be described.

(Received January 13, 1994; revised March 16, 1994)

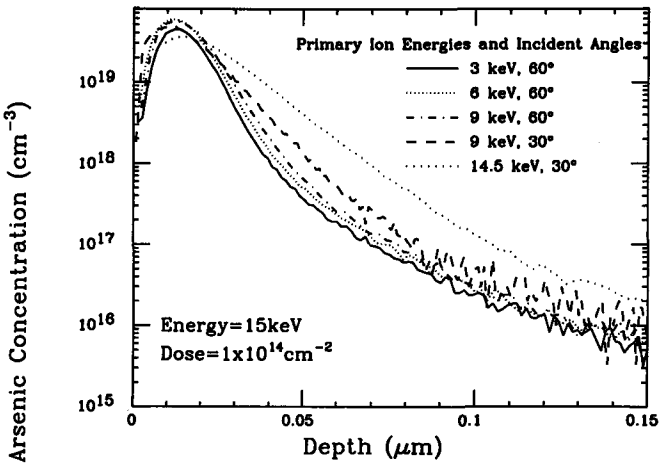

Fig. 1. An arsenic as-implanted profile implanted with 15 keV energy at 8° tilt angle and 22° rotation angle and measured by SIMS using different primary ion energies ranging from 3 keV to 14.5 keV, and primary ion incidence angles at 30 or 60° (relative to the surface normal.)

EXPERIMENTAL DETAILS

Ion Implantation

In order to understand the dependence of arsenic as-implanted profiles on the tilt and rotation angles as well as on dose and energy, 180 125 mm, (100) single-crystal silicon wafers were implanted with ^{75}As at implant energies of 15, 30, 50, 100, and 180 keV. Doses ranged from 1×10^{13} cm^{-2} to 8×10^{15} cm^{-2} and a wide range of implant angles were used by implanting with an Eaton NV 6200AV ion implanter. The wafers had a thin native oxide on top of the surface, estimated to be about 1.0 nm thick. Also, 5 100 mm (100) single-crystal wafers were prepared with a deposited amorphous Si layer 0.6 μm thick. These 100 mm wafers were used for arsenic implants into an amorphous layer for comparison with the implants into (100) single-crystal silicon. Since the NV 6200AV implanter uses an electrostatic-scanning system, many different combinations of tilt and rotation angles are generated on each wafer, and only at the center of the wafer does the ion beam enter the wafer at the nominal (specified) tilt and rotation angles. At other points on the wafer, the implant angles are offset by an amount depending on the configuration of the implanter and the location on the wafer. The nominal implant angles were carefully chosen in order to thoroughly observe the entire implant angle space of 0 to 10° of tilt, the angle between the normal to the wafer surface and the ion beam, and 0° to 360° of rotation, the angle the wafer is rotated about the normal to the surface. These ranges of angles were selected because most implants in semiconductor manufacturing lie within these bounds. Due to the eightfold symmetry of (100) single-crystal silicon, only rotation angles from 0° to 45° are needed in order to observe the entire rotation angle range. The location on the wafer was carefully correlated to the actual beam incident angle. The implanted wafers were diced into 4 × 4 mm samples for secondary ion mass spectroscopy (SIMS) analysis, which generated over 700 samples on each wafer representing implants at many different combinations of tilt and rotation angles. During the implantation, the beam current was intentionally set low so that the wafer temperature would not rise by more than 30°C. This circumvents the need to use gas cooling in most cases and helps to avoid the slight bowing of the wafers (the bowing occurs because of clamping during wafer cooling), which can result in a small shift in the actual ion beam incidence angle. However, for arsenic implants with higher doses, gas cooling had to be used in order to keep the wafer temperature from increasing, and to preserve the damage generated by implanted ions. In this case, since such heavy doses are sufficient to amorphize the single-crystal silicon, the profile dependence on implant angle is usually very small.

Another possible source of error in the implant angle is the wafer crystal cut error, which can change the actual beam incidence angle. The definition of wafer crystal cut error in <100> orientation wafers is the angle between the wafer's surface normal and the direction of the <100> axis. Thermal wave maps[1] of very low dose, high energy, normal incidence (0° tilt angle) ^{11}B implants on two wafers out of each 25 wafers were used to examine the location of minimum damage. This corresponds to the <100> direction, and the crystal cut error was determined to be less than 0.2° for the wafers used in this study.

Selection of SIMS parameters and SIMS Analysis

In order to understand and model the dependence of the as-implanted arsenic profiles on tilt and rotation angles as well as on dose and energy, over 400 arsenic implanted depth profiles were examined. The selection of the tilt and rotation angle combinations in the implant parameter space were optimized (minimal number of points providing the maximum amount of information) by observing the profile dependence on these implant parameters. Samples with implant energies of 15, 50, 100, 180 keV and doses of 1×10^{13}, 3×10^{13}, 1×10^{14}, 5×10^{14}, 2×10^{15}, and 8×10^{15} were selected.

Although SIMS analysis is a very accurate tool for depth profiling, an improper choice of measurement parameters can result in large errors in the measurements. A detailed discussion of these parameters, such as primary ion species, primary ion energy, and primary ion beam incident angle, and their impact on the accuracy of the measured profiles can be found in Ref. 2. Also, several practical considerations need to be understood concerning depth profiling with SIMS. For instance, issues such as profile broadening, surface roughening, primary ion beam incident angle, and secondary ion yield transients need to be understood. Using Cs^+ as the primary ion in SIMS analysis for arsenic profiles offers a better dynamic range compared to using O_2^+. However, it is well known that measuring shallow arsenic implanted

profiles with Cs^+ ion bombardment can cause severe profile broadening and can degrade the accuracy of the measurements[3,4] if care is not taken to select an appropriate set of SIMS parameters. For this reason, care was taken to obtain the optimal primary ion energy and the primary ion beam incident angle in order to suppress this adverse effect. Since profile broadening is caused by the momentum and energy transfer between the primary ions and the target atoms, it is a strong function of the primary ion energy and the primary ion beam incident angle.[5] In order to obtain the optimized primary ion energy and incident angle for measuring shallow arsenic implanted profiles, samples from the same implant condition were measured with several primary ion energies ranging from 3 keV to 14.5 keV and two different ion beam incident angles (30 and 60° from the surface normal). Figure 1 shows an arsenic implanted profile for 15 keV implant energy and 2×10^{14} cm^{-2} dose, measured with different Cs^+ primary ion energies and incident angles. The profile broadening can be observed clearly, and it can be seen to seriously degrade the accuracy of the measured profile. Figure 2 shows an arsenic as-implanted profile with 100 keV implant energy measured with two different primary ion energies. As can be seen, in this case the measured profile using a 14.5 keV primary ion energy agrees very well with the measured profile using a 6 keV primary ion energy. This is because profile broadening is a linear process with respect to the Cs^+ primary ion energy; thus the errors caused by it are relatively small compared with the much deeper profile of a higher energy implant.[3,4] Based on these observations, a primary ion energy of 14.5 keV was used for implanted profiles with an implant energy equal to or higher than 50 keV. It should be noted that the difference in the measured profiles in the tail region of the profile in this special case is due to the non-optimized setup of the instrument, and this results in a less sensitive detection limit. However, for measured profiles used in the model development, the instrument setup was optimized and has successfully provided better dynamic range.

The arsenic implanted profiles with implant energies higher than 50 keV were measured using Cs^+ primary ion bombardment with negative secondary ion mass spectrometry on a single CAMECA IMS-3f instrument. A nominal beam current of 0.3 μA was used. The primary ion beam was rastered over an area of either 250 or 350 μm^2, depending on the sputtering rate desired. The detected secondary ions were extracted from a central area either 15 or 30 μm in diameter in the center of the sputtered crater. Arsenic was monitored as the molecular ion $(As+Si)^-$ for enhanced sensitivity. The secondary ion counts were converted into concentration based on relative sensitivity factors. The conversion of sputtering time to depth is based on the measurement of the analytical craters using a Tencor stylus profilometer and should be accurate to within 10%.

The profiles implanted with energies of <50 keV are measured on a single Perkin Elmer 6600 secondary ion mass spectrometer, using Cs^+ primary ion bombardment with a net impact energy of 6 keV and an incident angle of 60° from the normal of the sample surface. The beam current was controlled at 180 nA. The primary ion beam was rastered over an area of either 300, 400, or 500 μm^2, depending on the sputtering rate desired. The secondary ions were collected from the central area with either 90, 120, or 150 μm on a side, respectively. The different raster sizes were required for the analysis due to the large difference in the depths of the implanted profiles for differing implant energies and widely varying degrees of channeling. The depths were established after the analysis by measuring the depths of the craters sputtered into samples with a calibrated profilometer. The overall accuracy of the profiles can be expected to be within 15%.

ANALYSIS OF THE ARSENIC AS-IMPLANTED PROFILES

In order to accurately model the profile variations (due to the variations in the degree of channeling and damage) as a function of tilt and rotation angles as well as dose and energy, a detailed study of the profile dependence on these implant parameters was undertaken. The results from this study are presented in this section.

Profile Dependence on Tilt and Rotation Angles

For all implant angle combinations, the measured profiles show significant channeling tails. This indicates that even for an implant angle combination that randomizes the incoming beam, significant channeling still occurs. This can be seen in Fig. 3, in which the implant into amorphous silicon has a much shallower depth. Near normal incidence, it is found that the effect of tilt angle is much stronger than that of rotation angle, and the channeling dependence on tilt

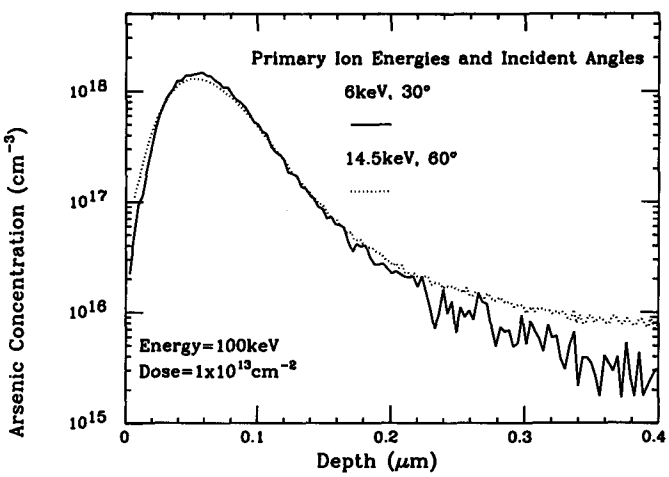

Fig. 2. An arsenic as-implanted profile implanted with 100 keV energy at 8° tilt angle and 22° rotation angle measured by SIMS using a Cs^+ primary ion energy of 6 keV with the primary ion incidence angle fixed at 30°, and a primary ion energy of 14.5 keV with the primary ion incidence angle fixed at 30°.

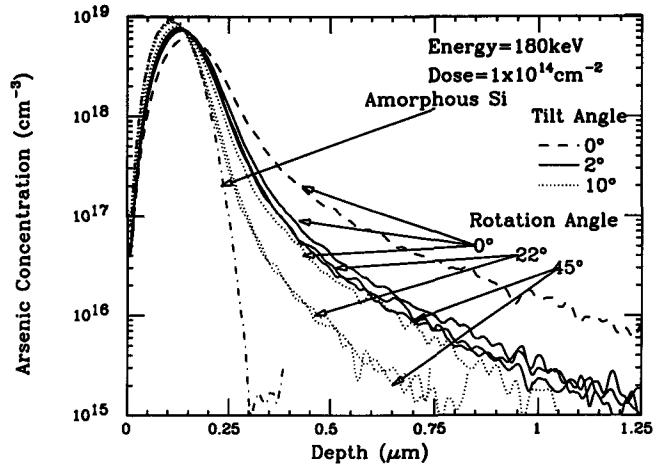

Fig. 3. Arsenic as-implanted profiles for various rotation angles with the tilt angle fixed at 0, 2, and 10°.

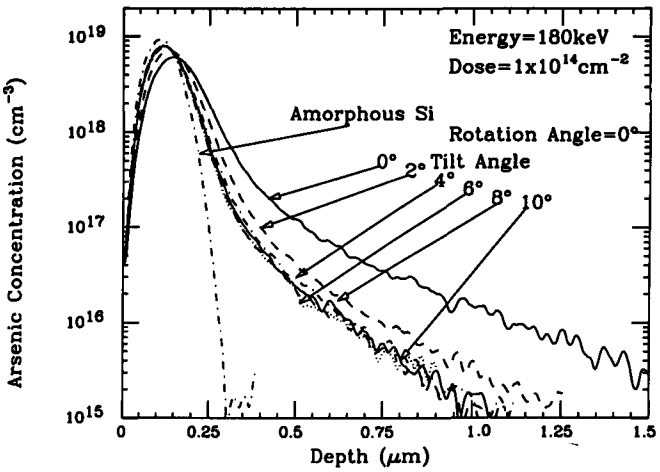

Fig. 4. Arsenic as-implanted profiles for various tilt angles with the rotation angle fixed at 0°.

angle is strongest. The effect of the rotation angle is observed to be relatively small in this case. However, the dependence of the profile on rotation is quite prominent at larger tilt angles where the profile has little or no dependence on tilt angle. Figure 3 shows the SIMS profiles for various rotation angles with the tilt angle fixed at 0, 2, and 10°.

Three channels have been observed to be the primary sources of major channeling of the incident ion beam. These are the <100> axial channel and the two {110} planar channels. Channeling was not observed in the two {100} planar channels, and this point will be discussed later. Other low index channels, such as the <110> and <111> axial channels are not major sources of channeling in these experiments, because a tilt angle of approximately 45° is necessary to direct the incoming ion beam into these channels.

As the tilt and rotation angles of the wafer are varied, the angle of the incident ion beam relative to the 'potential walls' of these three channels varies. The variation in the incident angle into these low index channels results in a variation in the amount of channeling with tilt and rotation angles. Figure 4 shows the SIMS profiles resulting from arsenic implants at 0° rotation and various tilt angles. One can see that as the tilt angle is increased above approximately 2 to 3° in the energy range of this study, the amount of channeling begins to decrease substantially. Figure 5 shows profiles at 8° tilt angle for various rotation angles and for an implant energy of 180 keV. The variation in channeling through the {110} planar channels can be observed in this figure as revealed by the greater degree of channeling at 0° rotation angle which exposes the {110} planar channels. For rotation angles greater than 10–15°, the profiles remain fairly constant with increasing rotation angles. This is illustrated in Fig. 5, where it can be seen that there is no dependence on rotation angle when the rotation angle exceeds 15°. A similar behavior is observed for implants at the other energies in the range 15–180 keV.

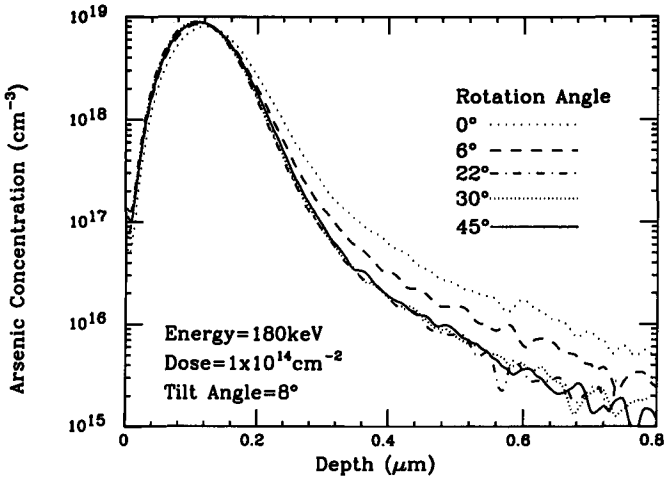

Fig. 5. Arsenic as-implanted profiles for various rotation angles with the tilt angle fixed at 8°.

Although 45° of rotation exposes the {100} planar channels to the ion beam, no measurable increase in channeling (or profile depth) has been observed in the range of energies studied in these measured profiles. This is believed to be due to the smaller physical size of the channel as seen by the incident ions; the small size of channel decreases the number and average distance of ions traveling through {100} channels. Thus, the effect of channeling through {110} planar channels is substantially greater than that through {100} planar channels. For this reason, this effect has not been observed within the limits of the accuracy of the SIMS data. The observed tilt and rotation angle channeling dependence is quite similiar to the previously reported dependence on tilt and rotation angle for implanted boron,[6] and BF_2.[7]

Profile Dependence on Dose and Energy

Figure 6 shows the measured SIMS profiles for four different energies at the same tilt and rotation angles as well as the same dose. As expected, the depth of the implanted profile increases monotonically as the implant energy increases. Figure 7 shows implant profiles of six different doses at 15 keV implant energy and with 10° tilt angle and 0° rotation angle. The

effect of the implant dose is well demonstrated here. The channeling component remains almost unchanged as the dose builds up, but the random scattering component (main concentration peak) increases rapidly as the dose increases. This is because as the dose increases, more and more damage is generated, which can very effectively shut down (or block) the channels in the crystal and begin to randomize the crystal structure.

MODEL EVALUATION

Simulations of implanted dopant profiles with semi-empirical models offer the advantage of being computationally efficient. This is very important as device structures and processes become more and more complicated. With the semi-empirical approach, the implant profiles are represented by analytical functions or combinations of several analytical functions with different parameters corresponding to different implant conditions. These parameters can be easily implemented into commercial process simulators in look-up tables and can be used to predict the implant dopant profiles of interest.

Due to the look-up table nature of this approach, most of the semi-empirical models available today are indeed computationally efficient. However, a lack of sufficient accuracy is still a problem for the currently available models. The first reason is that a single, simple analytical function which can effectively represent implant profiles of many extremely different implant conditions is difficult to establish. Gaussian,[8] Pearson,[8] and double Gaussian[9] functions have been used previously in many process simulators; however, these functions are found to be insufficient in describing the profile variations of extremely different implant conditions. This is due to the ion channeling effect which very significantly affects the profile shape in the tail region of the implant profile. Failure in modeling the channeling component usually results in a large discrepancy in the prediction of the profile depth.

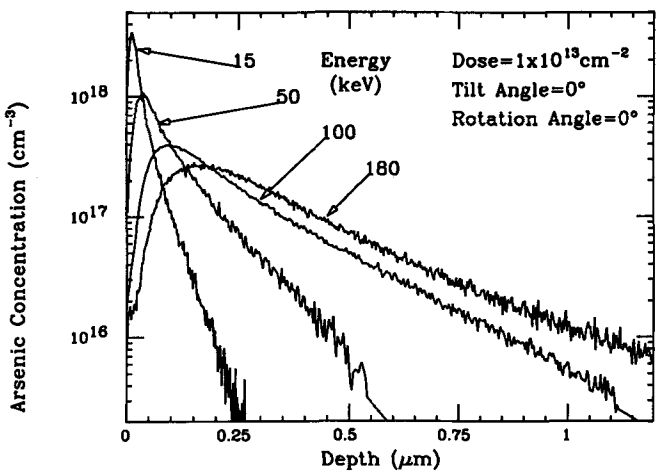

Fig. 6. Measured profile variation with energy for arsenic as-implanted profiles at a dose of 1×10^{13} cm^{-2} with the tilt and rotation angles fixed at 0°.

Recently, Tasch et al.[10,11] successfully demonstrated a new approach for accurate modeling for both boron and BF_2 implanted profiles with a Dual-Pearson function. The Dual Pearson is simply the sum of two Pearson distribution functions, one which accounts for the scattering component of the profile, and one accounting for the channeling component. Mathematically, it can be described by the equation

$$N(x) = r * f(x) + (1 - r) * g(x)$$

where N(x) is the normalized Dual Pearson, f(x) and g(x) are normalized Pearsons, and r describes the ratio between the Pearsons. Each Pearson function is in turn described by four parameters; namely, mean projected range (R_p), standard deviation (ΔR_p), skewness (γ), and kurtosis (β). Figure 8 illustrates an arsenic as-implanted profile modeled with the Dual-Pearson model.

PARAMETER EXTRACTION

In semi-empirical model development, the parameter extraction procedure must be carefully performed and can be very time consuming. Park et al.[12] developed an automatic parameter extraction code,

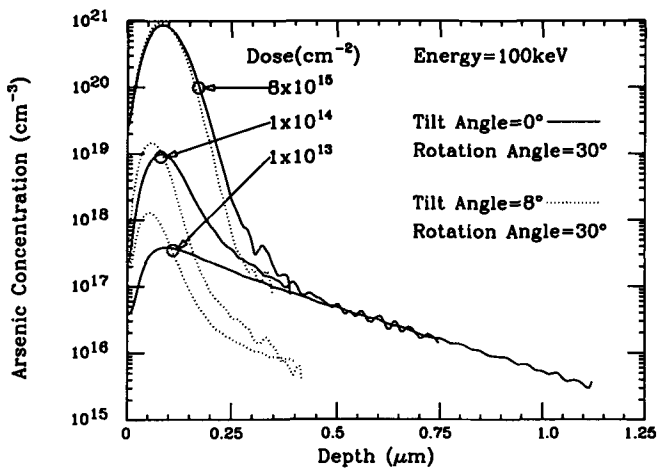

Fig. 7. Measured arsenic as-implanted profiles of various doses with tilt and rotation angle combinations of (0°, 30°), and (8°, 30°).

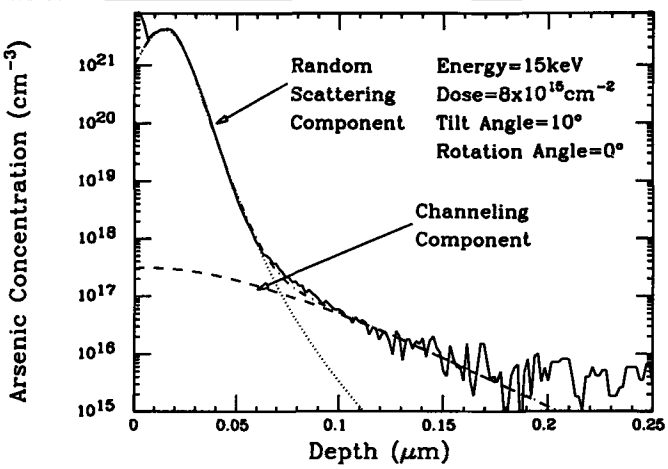

Fig. 8. Illustration of the application of the Dual-Pearson function to model arsenic implant profiles. The implant energy is 15 keV.

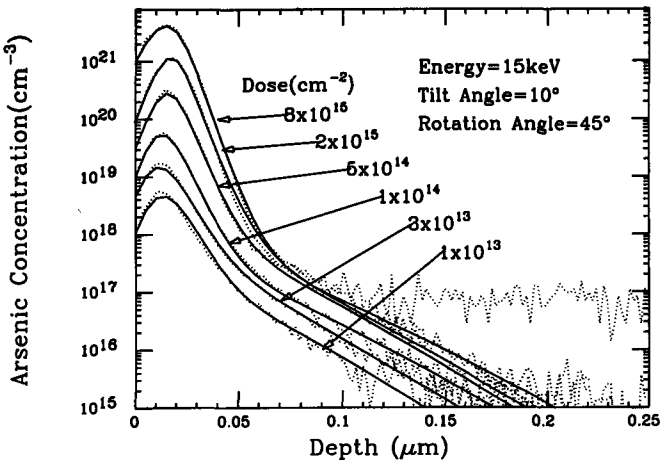

Fig. 9. Comparison of the simulated (solid curves) and experimentally measured (dotted curves) dose dependence of ion-implanted arsenic distributions in (100) silicon. The other implant parameters are held constant.

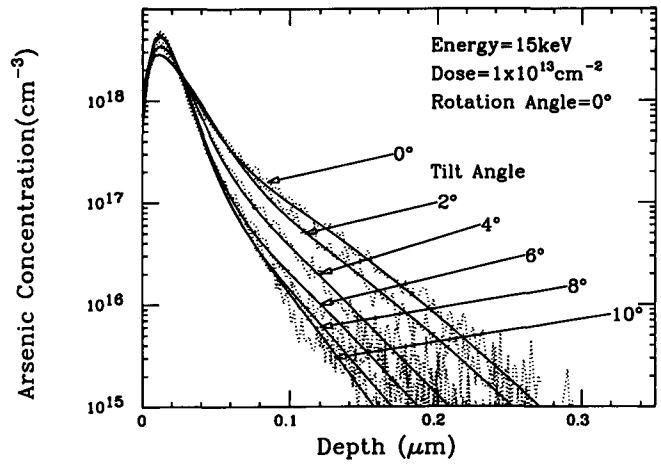

Fig. 10. Comparison of the simulated (solid curves) and experimentally measured (dotted curves) tilt angle dependence of ion-implanted arsenic distributions in (100) silicon.

Dual Pearson parameter extraction (DUPEX) to handle this problem. This code has been further enhanced by Morris as regards computational efficiency. The improved DUPEX version was adopted in extracting the Dual-Pearson parameters of arsenic implanted profiles. The nine Dual-Pearson parameters are extracted by a two-step process. The first step automatically generates a trial set of parameters, and these parameters are used as initial guess for the second step, which uses the Levenberg-Marquardt least squares fitting algorithm[13,14] to arrive at the final set of parameters which give the best fit to the arsenic distribution. In order to obtain accurate fits for both the channeling component and the random scattering component of the profile, two different weighting functions are used sequentially in parameter extraction. The first weighting function puts more emphasis on the peak region of the profile where the random scattering compnent dominates, while the second weighting function gives emphasis to the tail region of the profile where the channeling component is more important.

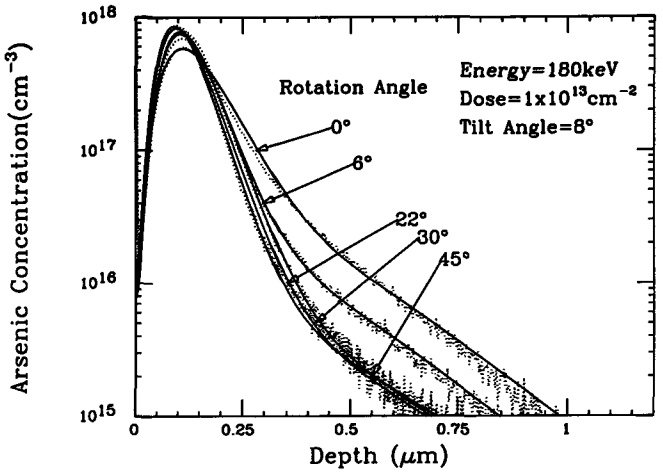

Fig. 11. Comparison of the simulated (solid curves) and experimentally measured (dotted curves) rotation angle dependence of ion-implanted arsenic distributions in (100) silicon.

After these parameters are extracted, they can be easily incorporated into a look-up table, and implemented in process simulators such as SUPREM III.[8,15]

IMPLEMENTATION IN SUPREM

The newly developed model for arsenic implants has been implemented in SUPREM III[8,15] in order to demonstrate the model capabilities, and because SUPREM III is very widely used in the industry. The model can be easily retrofit in other process simulators. The first step in the model implementation is to create the look-up table containing all of the available parameters which have been extracted from experimental data. The nine parameters of the Dual Pearson are listed in this table for each of four energies (15, 50, 100, and 180 keV), six doses (1×10^{13} cm^{-2}, 3×10^{13} cm^{-2}, 1×10^{14} cm^{-2}, 5×10^{14} cm^{-2}, 2×10^{15} cm^{-2}, and 8×10^{15} cm^{-2}), six tilt angles (0, 2, 4, °, 8, and 10°), and seven rotation angles (0, 6, 14, 22, 30, 38, and 45°). For implant conditions between those for which there is experimental data, an interpolation scheme is used. The interpolation between the parameters is done first for rotation angle, then tilt angle, then energy, in the order of increasing importance as regards the degree of dependence of the profile on the implant parameters. The interpolation for dose is done on a point-by-point basis, because the variation of the profile with dose, which occurs because of damage accumulation, can be very nonlinear. A linear interpolation between parameters does not work well, but a point-by-point interpolation reflects the trends properly. For example, for an implant with a 1×10^{15} cm^{-2} dose at a specific implant energy and implant angles, the new model will look in the look-up table for the two sets of parameters describing the next higher dose (2×10^{15} cm^{-2}) and the next lower dose (5×10^{14} cm^{-2}). With these two sets of parameters, two profiles as a function of depth are created first. The desired profile is then generated by interpolating the values of the two profiles described by the two sets of parameters.

This is done by interpolating the concentration at a specific depth with the two values of the the higher and lower dose profiles. Also, in areas where the profiles vary smoothly as a function of implant conditions, it is possible to extend the Dual-Pearson parameters beyond the region for which data was taken with a great degree of confidence. Thus, a four-phase interpolation scheme, along with the look-up table, allows a large range of implant conditions to be modeled: energies from 10 to 180 keV, any dose up to 10^{16} cm^{-2}, tilts from 0 to 10°, and any rotation angle (0° to 360°).

RESULTS AND DISCUSSIONS

The comparisons of the simulated arsenic distribution profiles with experimentally measured profiles as shown in Figs. 9, 10, and 11 demonstrate the self-consistency of this new model. The profile variation with dose due to the damage build-up is accurately simulated as shown in Fig. 9. Figures 10 and 11 demonstrate the accuracy of this model in simulating the profile dependence on tilt and rotation angles which is due to the variation in the amount of channeling. In order to illustrate the capability of the interpolation algorithm, Fig. 12 shows a comparison between a predicted profile generated by using the interpolation scheme in this new model and an experimentally measured profile. The comparison is made as follows: In the actual look-up table in the new model, there are model parameters in the look-up table for doses of 1×10^{13} cm^{-2}, 3×10^{13} cm^{-2}, and 1×10^{14} cm^{-2} for an implant energy of 15 keV, and tilt and rotation angles of 10 and 0°, respectively. Normally for doses between 1×10^{13} cm^{-2} and 3×10^{13} cm^{-2}, the interpolation algorithm would interpolate between these two dose points. However, in order to demonstrate the interpolation capability, the model parameters for 3×10^{13} cm^{-2} dose in the look-up table were *not* used. Instead, the interpolation was performed between the two dose points 1×10^{13} cm^{-2} and 1×10^{14} cm^{-2} in order to generate the profile for the 3×10^{13} cm^{-2} dose. This is a stronger test of the interpolation algorithm. Then the simulated profile was compared with the experimental SIMS data. The dotted line in Fig. 12 is the experimentally measured profile, and the solid line is the simulated profile generated by interpolation. This figure shows very good agreement between the predicted profile using interpolation and the experimental data. Since the dose points in the look-up table are much closer (3X) together, the accuracy of the dose interpolation scheme is expected to be better than what is shown in this figure.

The significant improvement of this new model is illustrated by Fig. 13, which compares the predictions of the new model with the existing SUPREM III[8] implant depth profile model. In this figure, the experimental data are represented by the dotted lines. The predictions of the new model are denoted by the solid line, and the predictions of the existing SUPREM III[8] model are denoted by the dot-dash lines. It is not

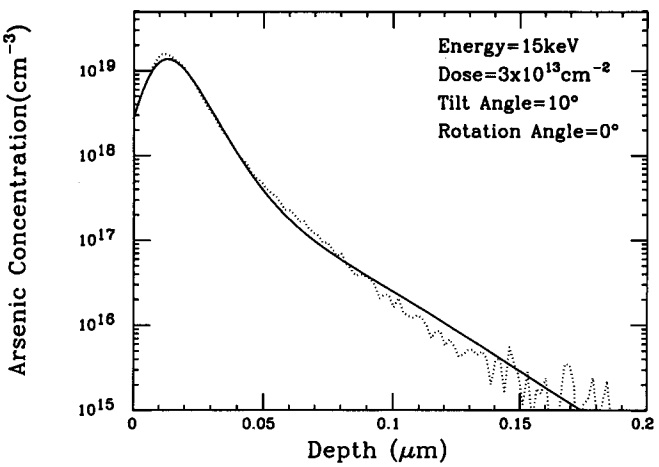

Fig. 12. Comparison of the simulated profile using the interpolation algorithm in the new model with the experimentally measured SIMS profile for a 15 keV implant. The solid line is the predicted profile, and the dotted line represents the experimentally measured profile.

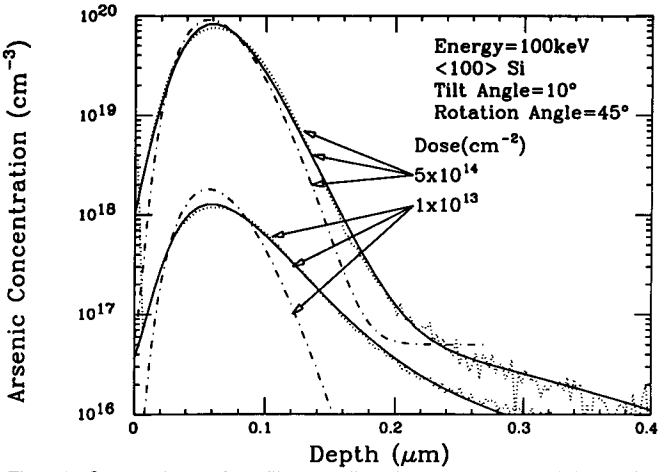

Fig. 13. Comparison of profiles predicted by the new model and the previous model in SUPREM III. The solid lines are profiles predicted by the new model, and the dot-dashed lines are prediction from the previous model. The experimentally measured profiles are represented by the dotted lines.

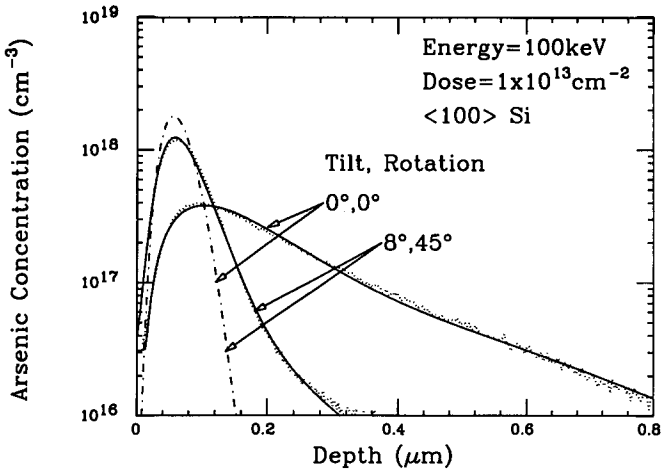

Fig. 14. Comparison of profiles predicted by the new model and the previous model in SUPREM III. The solid lines are profiles predicted by the new model, and the dot-dashed lines are prediction from the previous model. The experimentally measured profiles are represented by the dotted lines.

surprising that the existing SUPREM III[8] model does not show any dependence on the implant angle, since it is calculated with LSS theory which assumes an amorphous target. Also, since the existing SUPREM III[8] model assumes an amorphous target, channeling tails are neglected, and the shape of the profile does not change even as the implant dose increases. This can be seen in Fig. 14. It is evident from these figures that the new model provides considerably more accurate results than does the existing SUPREM III[8] model.

CONCLUSIONS

In conclusion, we have performed an extensive study of the dependence of the arsenic as-implant profiles on tilt angle, rotation angle, dose and energy. Over 400 SIMS extracted profiles have been examined, which cover a very wide range of implant conditions. The explicit dependencies of the profiles on the implant conditions were examined in close detail, and the three primary sources of channeling for this range of implant parameters were found to be the <100> axial channel and the two {110} planar channels. Based on this knowledge, an accurate and computationally efficient model for the simulation of arsenic as-implanted profiles into single-crystal (100) silicon for the implant conditions covered was developed. This model utilizes the Dual-Pearson function to describe the arsenic dopant distributions. Parameters were extracted for all of the experimental data and a look-up table was created to contain this information. The model has been implemented in SUPREM III with the use of this look-up table and a four-phase interpolation scheme. The implemented model covers the following range of implant conditions: energies from 10 to 180 keV, any dose up to 10^{16} cm^{-2}, tilts from 0 to 10°, and any rotation angle (0 to 360°). Although the model is based on experimental data with doses of up to approximately 10^{16} cm^{-2}, it is believed that the model can represent higher doses with reasonable accuracy. This is due to the nature of the profile dependence on dose. A typical simulation with this model takes only seconds on a workstation. This newly developed model very largely improves the ability to accurately simulate as-implanted arsenic profiles for a wide range of implant parameters. Its use can aid significantly in more efficient technology development, improved understanding of implant process control issues, and the development of improved diffusion models for arsenic implants for the range of implant parameters covered in this work.

ACKNOWLEDGMENTS

This work was supported in part by SEMATECH, the Semiconductor Research Corporation, Motorola, Intel, Texas Instruments, and Advanced Micro Devices.

REFERENCES

1. W.L. Smith, A. Rosenwaig, D. Willenborg, J. Opsal and M.W. Taylor, *Solid State Technol.* 29, 85 (1986).
2. R.G. Wilson, F.A. Dtevie and C.W. Magee, *Secondary Ion Mass Spectrometry,* (New York: John Wiley & Sons, 1989).
3. W. Vandervorst, H.E. Maes and R.F. De Keersmaecker, *J. Appl. Phys.* 56, 1425 (1984).
4. J.J. Lee, J.E. Fulghum, G.E. McGuire, M.A. Ray, C.M. Osburn and R.W. Linton, *J. Vac. Sci. Technol. A* 8, 2287 (1990).
5. K. Wittmaack and W. Wach, *Nucl. Instrum. Meth.* 191, 327 (1981).
6. K.M. Klein, C. Park, A.F. Tasch, B. Simonton and S. Novak, Electrochem. Soc. Spring Mtg., *Ext. Abstracts,* 357 (1990).
7. P. Gupta, C. Park, K. Klein, S. Yang, S. Morris, V. Do, *Proc. Mater. Res. Soc.* 1991 Fall Mtg. (1991).
8. C. Ho, S. Hansen and P. Fahey, *Stanford University Technical Report* (1984).
9. L.C. Chien, S. Corcoran, M. Taylor, A. Chatterjee, J. Garcia and R. Mathur, *Proc. Second Intl. Workshop on the Measurement and Characterzation of Ultra-Shallow Doping Profiles in Semiconductors* (1993).
10. A.F. Tasch, H. Shin, C. Park, J. Alvis and S. Novak, *J. Electrochem. Soc.* 136, 810 (1989).
11. S.J. Morris, V. Do, P. Gupta, S. Yang, C. Park, K.M. Klein and A.F. Tasch, Electrochem. Soc. Spring Mtg., *Ext. Abstracts,* 92-1, 450 (1992).
12. C. Park, K.M. Klein and A.F. Tasch, *Solid State Electronics* 33, 645 (1990).
13. K. Levenberg, *Quart., Appl., Math.* 2, 164 (1944).
14. D. Marquardt, *SIAM J. Appl. Math.* 11, 431 (1963).
15. C. Park, Ph. D. dissertation, The University of Texas at Austin, Austin (1991).